

A COMPREHENSIVE NOTE ON THERMALLY STRATIFIED FLOW AND NON-FOURIER HEAT FLUX THEORY

by

**Muhammad Ijaz KHAN^{a*}, Muhammad WAQAS^b,
Tasawar HAYAT^{a,c}, and Ahmed ALSAEDI^c**

^a Department of Mathematics, Quaid-I-Azam University, Islamabad, Pakistan

^b NUTECH School of Applied Sciences and Humanities, National University of Technology,
Islamabad, Pakistan

^c Nonlinear Analysis and Applied Mathematics Research Group,
Department of Mathematics, Faculty of Science, King Abdulaziz University, Jeddah, Saudi Arabia

Original scientific paper
<https://doi.org/10.2298/TSCI171126140K>

Here an analysis is presented to investigate the characteristics of non-Fourier flux concept in flow induced by stretching cylinder. Unlike the convectional approach, the heat flux by Cattaneo-Christov theory is considered. Stagnation point flow in the presence of thermal stratification and temperature dependent thermal conductivity is addressed. Rheological properties are examined for hyperbolic tangent material. Theory of the boundary-layer is implemented for the formulation purpose. The relevant transformations yield the strong non-linear differential systems which are numerically computed. Plots are presented for the solution expressions of velocity and temperature. Surface drag force is calculated and discussed. Here velocity and temperature are enhanced for the larger curvature parameter. Larger values of thermal relaxation factor give rise to be decrease in temperature.

Key words: *non-Fourier heat flux theory, thermally stratified medium, variable properties, hyperbolic tangent liquid*

Introduction

The transport phenomenon of non-Newtonian materials emerges in several branches of chemical, materials, and mechanical engineering. These materials illustrate shear stress/strain association which deviate considerably from the conventional Newtonian model *i. e Navier-Stokes model*. Different models for non-Newtonian materials comprise few adjustments in momentum conservation expressions [1-10]. Hyperbolic tangent four constants fluid is one of such models which can describe the shear thinning properties. This model is interpreted through the kinetic concept of liquids instead of empirical relation. Apparent viscosity of hyperbolic tangent fluid varies between zero to infinity. Moreover, this model has several advantages over other models including the ease of computation, simplicity and physical robustness. Some recent flow investigations involving hyperbolic tangent liquid and other fluids models are given through [11-20] and many studies therein.

Theory of heat conduction established by Fourier [20] communicates heat flux in a direct manner with temperature gradient utilizing coefficient of thermal conductivity. Under cer-

* Corresponding author, e-mail: mikhan@math.qau.edu.pk

tain circumstances the Fourier relation is authentic enough for distinct engineering problems apart from the problems which incorporate relatively higher temperature gradient, nano and micro scales in space and time, absolute null temperatures and small variation in temperature [21, 22]. Several non-Fourier conduction concepts have been presented to determine these issues. The situations in microelectronic mechanisms including combined circuit chips, laser pulses heating of high rate or heat flux via cutting and melting of materials and in few non-homogeneous materials, the non-Fourier conduction is very significant [23-26]. Thus some numerical and analytical investigations regarding non-Fourier conduction have been presented in literature. For instance Straughan [27] explored thermal convection in non-Fourier flux model. Uniqueness of non-Fourier flux for incompressible flow liquids is investigated by Tibulle *et al.* [28]. Han *et al.* [29] reported the non-Fourier flux features in stretched flow of Maxwell material. Analysis presented in [29] is further extended by Hayat *et al.* [30] by considering non-Fourier flux and variable thickness of sheet. Khan *et al.* [31] established analytical solutions for 3-D stretched flow of Burgers material in presence of different chemical processes and non-Fourier flux. Effectiveness of thermal stratification in variable thermal conductivity stretched flow of viscous and Eyring-Powell materials is addressed by Hayat *et al.* [32, 33]. Ali *et al.* [34] examined radiation and MHD characteristics in Casson ferrofluid. Non-Fourier flux consideration in Maxwell nanoliquid flow with slip aspect is presented by Sui *et al.* [35]. Nadeem *et al.* [36] considered non-Fourier flux and stratification phenomenon in flow by Maxwell nanomaterial.

Thermal stratification is regarded a renowned device of biogeochemical series in lakes [37-39]. Strong stratification decelerates the avoids of transfer of elements within surface and ground waters. Consequently, the regulating methods and subsequent water excellence in small citified pond bionetworks would possibly be influenced by the time and strength of temperature stratification. However communication between physical and biogeochemical procedures (for example temperature stratification) in citified pond bionetworks remain badly studied. Our intention here is to explore stratification characteristics in variable thermal conductivity stretched flow of hyperbolic tangent material. Flow caused here is due to stretching cylinder. Some investigations regarding laminar and turbulence flow can be mentioned through [40-47]. Solutions of non-linear system are obtained numerically through bvp4c technique. Graphical demonstrations for diverse influential variables against velocity and temperature distributions are further motivation of this investigation.

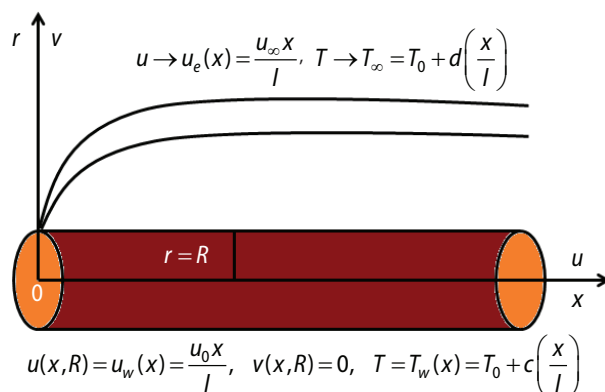


Figure 1. Geometry of flow problem

fer process is based using non-Fourier heat flux. Governing flow expressions for hyperbolic tangent liquid [27]:

Formulation

Flow equations

Here 2-D stagnation point flow of incompressible hyperbolic tangent material towards stretched cylinder with velocity $u_w(x) = u_0(x/l)$ is investigated, see fig. 1.

The free stream velocity is denoted by u_e . Heat generation/absorption and dissipation effect are neglected. Heat transfer process is in the absence of heat source/sink and viscous dissipation effect. Heat trans-

$$\frac{\partial(ru)}{\partial x} + \frac{\partial(rv)}{\partial r} = 0 \quad (1)$$

$$u \frac{\partial u}{\partial x} + v \frac{\partial u}{\partial r} = \nu(1-n) \left(\frac{\partial^2 u}{\partial r^2} + \frac{1}{r} \frac{\partial u}{\partial r} \right) + n\sqrt{2}\Gamma \nu \frac{\partial u}{\partial r} \frac{\partial^2 u}{\partial r^2} + \frac{n\Gamma}{2} \nu \left(\frac{\partial u}{\partial r} \right)^2 + u_e(x) \frac{du_e(x)}{dx} \quad (2)$$

with

$$u(x, R) = u_w(x) = \frac{u_0 x}{l}, \quad v(x, R) = 0 \quad (3)$$

$$u(x, r) \rightarrow u_e(x) = \frac{u_\infty x}{l} \quad \text{as } r \rightarrow \infty$$

In the aforesaid expressions (u, v) signify the velocity components in (x, r) directions, respectively, ν – the kinematic viscosity, ρ – the density of the liquid, Γ – the material parameter, n – the power index, and (u_w, u_e) the stretching and free stream velocities, respectively. In view of the transformations:

$$\eta = \sqrt{\frac{u_0}{\nu l}} \left(\frac{r^2 - R^2}{2R} \right), \quad u = \frac{u_0 x}{l} f'(\eta), \quad v = -\frac{R}{r} \sqrt{\frac{u_0 \nu}{l}} f(\eta) \quad (4)$$

Equation (1) is justified automatically whereas eqs. (2) and (3) are converted to the following forms:

$$(1-n)(1+2\gamma\eta) f''' + 2\gamma(1-n) f'' + ff'' - f'^2 + 2\lambda n(1+2\gamma\eta)^{3/2} f''f''' + 3\lambda\gamma(1+2\gamma\eta)^{1/2} (f'')^2 + A^2 = 0 \quad (5)$$

$$f(0) = 0, \quad f'(0) = 1 \quad \text{and} \quad f'(\infty) = A \quad (6)$$

where $\lambda = (\Gamma u_0^{3/2} x) / [(2\nu)^{1/2} l^{3/2}]$ denotes the Weissenberg number, $A = u_\infty / u_0$ the ratio of velocities, and $\alpha = [(\nu l) / (u_0 R^2)]^{1/2}$ the curvature parameter.

Energy equation

The energy equation for this case is:

$$\rho c_p \left(u \frac{\partial T}{\partial x} + v \frac{\partial T}{\partial r} \right) = -\bar{\nabla} \cdot \bar{\mathbf{q}} \quad (7)$$

where T is the temperature, c_p – the specific heat, and $\bar{\mathbf{q}}$ – the heat flux. Heat flux in view of Cattaneo-Christov expression satisfies:

$$\bar{\mathbf{q}} + \lambda_1 \left(\frac{\partial \bar{\mathbf{q}}}{\partial t} + \bar{\mathbf{v}} \bar{\nabla} \cdot \bar{\mathbf{q}} - \bar{\mathbf{q}} \bar{\nabla} \cdot \bar{\mathbf{v}} + (\bar{\nabla} \cdot \bar{\mathbf{v}}) \bar{\mathbf{q}} \right) = -k(T) \bar{\nabla} T \quad (8)$$

where λ_1 denotes the thermal relaxation time of heat flux and $k(T)$ the temperature dependent thermal conductivity. For $\lambda_1 = 0$, eq. (8) reduces to Fourier's law. Equation (8) for incompressibility condition yields:

$$\bar{\mathbf{q}} + \lambda_1 (\bar{\mathbf{v}} \nabla \bar{\mathbf{q}} - \bar{\mathbf{q}} \nabla \bar{\mathbf{v}}) = -k(T) \nabla T \quad (9)$$

Eliminating $\bar{\mathbf{q}}$ from eqs. (7) and (9) we obtain:

$$u \frac{\partial T}{\partial x} + v \frac{\partial T}{\partial r} + \lambda_1 \left(u^2 \frac{\partial^2 T}{\partial x^2} + v^2 \frac{\partial^2 T}{\partial r^2} + 2uv \frac{\partial^2 T}{\partial r \partial x} + u \frac{\partial u}{\partial x} \frac{\partial T}{\partial x} + u \frac{\partial v}{\partial r} \frac{\partial T}{\partial r} + v \frac{\partial u}{\partial r} \frac{\partial T}{\partial x} + v \frac{\partial v}{\partial r} \frac{\partial T}{\partial r} \right) = \frac{1}{\rho c_p r} \frac{\partial}{\partial r} \left[k(T) r \frac{\partial T}{\partial r} \right] \quad (10)$$

with the conditions:

$$T = T_w(x) = T_0 + c \left(\frac{x}{l} \right) \quad \text{at } r = a \quad (11)$$

$$T = T_\infty(x) = T_0 + d \left(\frac{x}{l} \right) \quad \text{when } r \rightarrow \infty$$

where (c, d) denotes the dimensional constants and (T, T_0, T_∞) the fluid, reference and ambient temperatures, respectively. The temperature dependent thermal conductivity $k(T)$ is [24]:

$$k(T) = k_\infty \left(1 + \varepsilon \frac{T - T_\infty}{\Delta T} \right) \quad (12)$$

in which ε represents the small scalar parameter and k_∞ the thermal conductivity of the ambient fluid and $\Delta T = T_w - T_0$.

Employing:

$$\theta(\eta) = \frac{T - T_\infty}{T_w - T_0} \quad (13)$$

together with eq. (11) we have from eq. (10):

$$(1 + 2\gamma\eta)\theta'' + 2\gamma\theta' + \text{Pr}(f\theta' - f'\theta) + \varepsilon \left[\frac{(1 + 2\gamma\eta)}{(\theta'^2 + \theta\theta'')} + 2\gamma\theta\theta' \right] - \text{Pr} \delta f f' \theta' - \text{Pr} \delta f^2 \theta'' = 0 \quad (14)$$

$$\theta(0) = 1, \quad \theta(\infty) = 0 \quad (15)$$

where $\text{Pr} = \mu c_p / k$ shows the Prandtl number and $\gamma = \lambda_1 u_0 / l$ the thermal relaxation factor.

Physical quantity

Here skin friction coefficient is:

$$C_f = \frac{2\tau_w}{\rho u_w^2} \quad (16)$$

The wall shear stress at $r = R$ is:

$$\tau_w = \mu \left[(1-n) \frac{\partial u}{\partial r} + \frac{n}{\sqrt{2}} \Gamma \left(\frac{\partial u}{\partial r} \right)^2 \right]_{r=R} \quad (17)$$

From eqs. (16) and (17) one has:

$$\frac{C_f \text{Re}_x^{1/2}}{2} = (1-n)f''(0) + n\lambda f''^2(0) \quad (18)$$

In which Re_x denotes Reynolds number.

Solution methodology and analysis of results

Here bvp4c technique is employed in order to solve eqs. (5) and (14) together with boundary conditions (6) and (15). Our intention here is to analyze the characteristics of distinct physical variables like curvature parameter, γ , power index, n , Weissenberg number, λ , Prandtl number, thermal stratification parameter, S , variable thermal conductivity parameter, ε , and thermal relaxation parameter, δ , on dimensionless velocity, $f'(\eta)$, and temperature $\theta(\eta)$. Such objective is achieved via plots in figs. 2-11.

Figure 2 disclosed the impact of γ on $f'(\eta)$. Larger values of γ enhance the velocity. Physically radius of cylinder reduces when α is enhanced which offers little resistance to the fluid motion and consequently the fluid velocity increases. Effect of n on $f'(\eta)$ is depicted through fig. 3. Clearly larger n decay $f'(\eta)$ and related thickness of momentum layer. Analysis of characteristics of λ on $f'(\eta)$ is presented through fig. 4. Since Weissenberg number is the ratio of relaxation time of the fluid and a specific process time. It increases the thickness of the fluid due to which the velocity decays for larger λ .

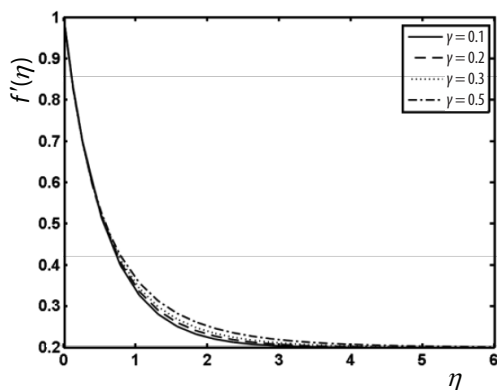


Figure 2. The $f'(\eta)$ via γ when $S = \delta = \varepsilon = 0.2$, $n = A = \lambda = 0.1$ and $\text{Pr} = 2.0$

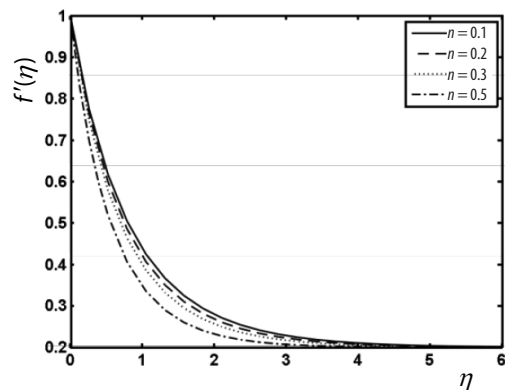


Figure 3. The $f'(\eta)$ via n when $S = \delta = \varepsilon = \gamma = 0.2$, $A = \lambda = 0.1$ and $\text{Pr} = 2.0$

Figure 5 reports the behavior of γ on $\theta(\eta)$. Clearly $\theta(\eta)$ decays near stretching cylinder however it increases far away from the surface. In fact, rise in γ causes an enhancement in thermal thickness of thermal layer. As a consequence, the heat transport rate reduces and therefore $\theta(\eta)$ of the liquid is higher. Salient features of n and λ on $\theta(\eta)$ are described via figs. 6 and 7. Here $\theta(\eta)$ is via enhancement of n . When n is enhanced however opposite behavior is noted for higher λ . Figure 8 signifies the impact of Prandtl number on $\theta(\eta)$. As expected $\theta(\eta)$ diminishes for higher values of Prandtl number since there is an inverse relationship between Prandtl number and thermal diffusivity. Due to this reason the temperature decays. Figure 9 elucidates the variation of S on $\theta(\eta)$. It is reported that $\theta(\eta)$ and related thermal layer are reduced when S increases. Physically larger S reduce the convective flow between ambient fluid and heated cylinder and therefore $\theta(\eta)$ reduces. Behavior of ε on $\theta(\eta)$ is scrutinized through

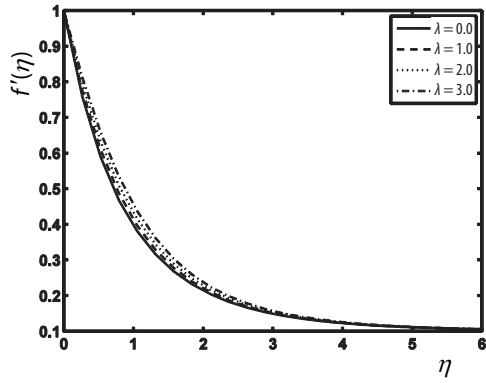


Figure 4. The $f'(\eta)$ via λ when $S = \delta = \varepsilon = \gamma = 0.2$, $A = n = 0.1$ and $Pr = 2.0$

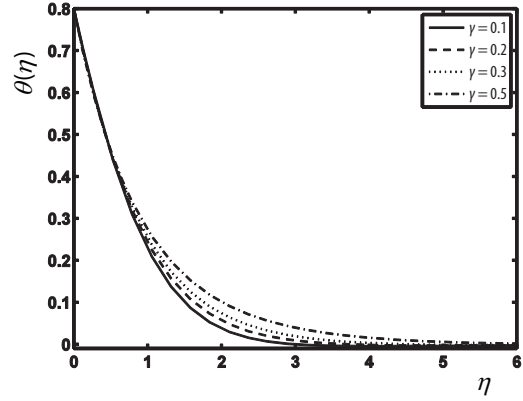


Figure 5. The $\theta(\eta)$ via γ when $S = \delta = \varepsilon = 0.2$, $A = n = \lambda = 0.1$ and $Pr = 2.0$

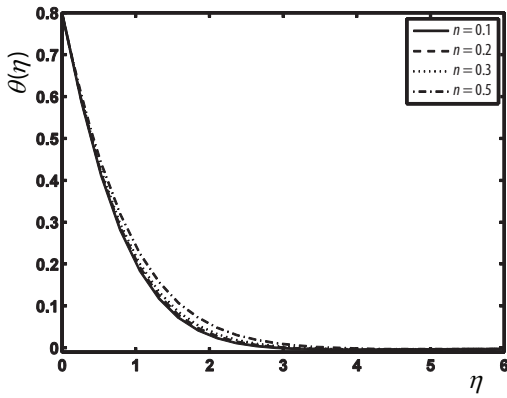


Figure 6. The $\theta(\eta)$ via n when $S = \delta = \varepsilon = \gamma = 0.2$, $A = \lambda = 0.1$ and $Pr = 2.0$

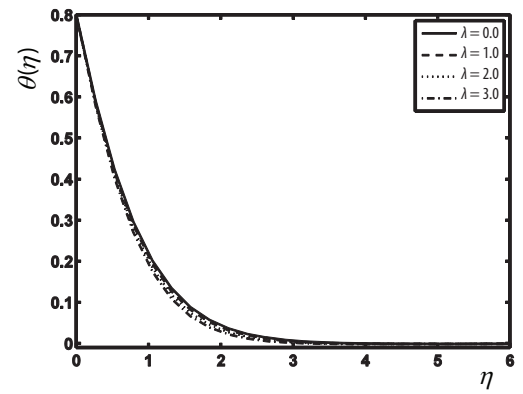


Figure 7. The $\theta(\eta)$ via λ when $S = \delta = \varepsilon = \gamma = 0.2$, $A = n = 0.1$ and $Pr = 2.0$

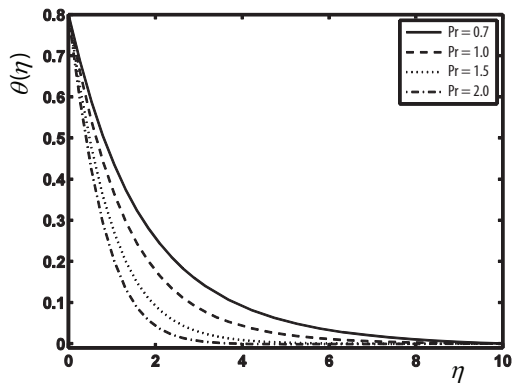


Figure 8. The $\theta(\eta)$ via Pr when $S = \delta = \varepsilon = \gamma = 0.2$, and $A = n = \lambda = 0.1$

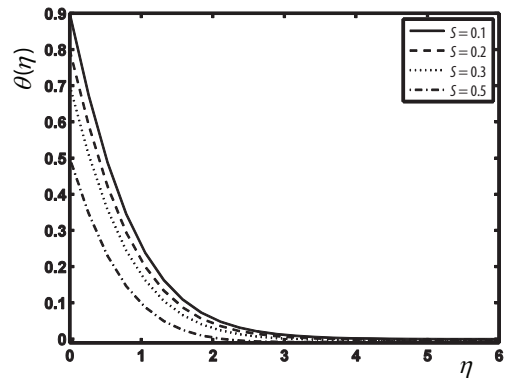


Figure 9. The $\theta(\eta)$ via S when $\delta = \varepsilon = \gamma = 0.2$, and $A = n = \lambda = 0.1$, and $Pr = 2.0$

fig. 10. Here $\theta(\eta)$ is an increasing function of ε . Physically thermal conductivity of the liquid increases for larger ε due to which more amount of heat is transferred from sheet to the fluid and thus temperature enhances. Figure 11 highlights the impact of δ on $\theta(\eta)$. Here temperature enhances via δ . Physically when we increase δ then material particles need extra time to transfer heat to its adjacent particles and so temperature reduces. For $\delta = 0$ the heat transfers promptly throughout the material. Hence temperature distribution is higher for $\delta = 0$ *i. e.* for Fourier's law when compared with Cattaneo-Christov heat flux model.

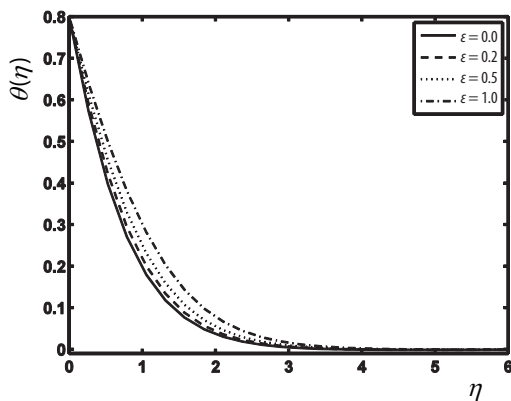


Figure 10. The $\theta(\eta)$ via ε when $\delta = S = \gamma = 0.2$, and $A = n = \lambda = 0.1$ and $Pr = 2.0$

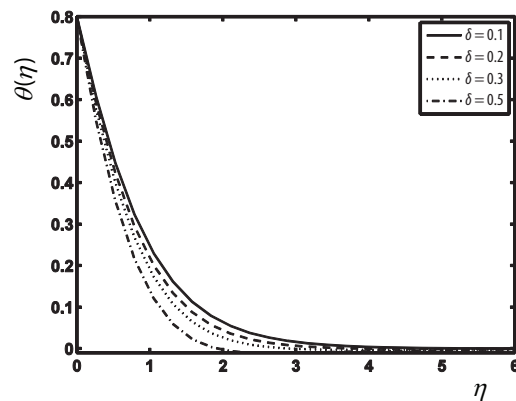


Figure 11. The $\theta(\eta)$ via δ when $\varepsilon = S = \gamma = 0.2$, and $A = n = \lambda = 0.1$ and $Pr = 2.0$

Table 1 explores characteristics of n , γ , λ , and A on skin friction ($C_f Re_x^{1/2}$) when $\varepsilon = S = \delta = 0.2$ and $Pr = 2.0$. Here $C_f Re_x^{1/2}$ rises via larger γ whereas it decays for n , λ and A .

Table 1. Numerical data for skin friction ($C_f Re_x^{1/2}$) when $\varepsilon = S = \delta = 0.2$ and $Pr = 2.0$

n	γ	λ	A	$C_f Re_x^{1/2}$
0.1	0.2	0.1	0.1	-0.9625799
0.2				-0.8981956
0.3				-0.8287302
0.5				-0.6655272
0.1	0.1			-0.9395822
	0.2			-0.9625799
	0.3			-0.9848631
	0.5			-1.0274700
	0.2	0.0		-0.9839514
		1.0		-0.787906
		2.0		-0.6319903
		3.0		-0.5141813
		0.1	0.1	-0.9625799
			0.2	-0.9122701
			0.3	-0.844517
			0.4	-0.7614328

- [10] Waqas, M., et al., Magnetohydrodynamic (MHD) Mixed Convection Flow of Micropolar Liquid Due to Nonlinear Stretched Sheet with Convective Condition, *International Journal of Heat and Mass Transfer*, 102 (2016), Nov., pp. 766-772
- [11] Hayat, T., et al., Impact of Cattaneo-Christov Heat Flux Model in Flow of Variable Thermal Conductivity Fluid over a Variable Thickened Surface, *International Journal of Heat and Mass Transfer*, 99 (2016), Aug., pp. 702-710
- [12] Hayat, T., et al., Stagnation Point Flow with Cattaneo-Christov Heat Flux and Homogeneous-Heterogeneous Reactions, *Journal of Molecular Liquids*, 220 (2016), Aug., pp. 49-55
- [13] Khan, M. I., et al., A Comparative Study of Casson Fluid with Homogeneous-Heterogeneous Reactions, *Journal of Colloid and Interface Science*, 498 (2017), July, pp. 85-90
- [14] Hayat, T., et al., Entropy Generation in Flow with Silver and Copper Nanoparticles, *Colloids and Surfaces A: Physicochemical and Engineering Aspects*, 539 (2018), Feb., pp. 335-346
- [15] Hayat, T., et al., Entropy Generation in Magnetohydrodynamic Radiative Flow Due to Rotating Disk in Presence of Viscous Dissipation and Joule Heating, *AIP, Physics of Fluids*, 30 (2018), 1, 017101
- [16] Khan, M. I., et al., Activation Energy Impact in Nonlinear Radiative Stagnation Point Flow of Cross Nanofluid, *International Journal of Heat and Mass Transfer*, 91 (2018), Feb., pp. 216-224
- [17] Khan, M. I., et al., Significance of Nonlinear Radiation in Mixed Convection Flow of Magneto Walter-B Nanofluid, *International Journal of Hydrogen Energy*, 42 (2017), 42, pp. 26408-26416
- [18] Khan, W. M. A., et al., Entropy Generation Minimization (EGM) of Nanofluid Flow by a Thin Moving Needle with Nonlinear Thermal Radiation, *Physica B: Condensed Matter*, 534 (2018), Apr., pp. 113-119
- [19] Hayat, T., et al., Magnetohydrodynamic Flow of Burgers Fluid with Heat Source and Power Law Heat Flux, *Chinese Journal of Physics*, 55 (2017), 2, pp. 318-330
- [20] Fourier, J. B. J., *Theorie Analytique De La chaleur*, F. Didot, Paris, 1822
- [21] Qayyum, S., et al., Comparative Investigation of Five Nanoparticles in Flow of Viscous Fluid with Joule Heating and Slip Due to Rotating Disk, *Physica B: Condensed Matter*, 534 (2018), Apr., pp. 173-183
- [22] Lam, T. T., et al., Application of Solution Structure Theorem to Non-Fourier Heat Conduction Problems: Analytical Approach, *International Journal of Heat and Mass Transfer*, 54 (2011), 23-24, pp. 4796-4806
- [23] Daneshjou, K., et al., Non-Fourier Heat Conduction Analysis of Infinite 2D Orthotropic FG Hollow Cylinders Subjected to Time-Dependent Heat Source, *Applied Thermal Engineering*, 98 (2016), Apr., pp. 582-590
- [24] Cattaneo, C., A Form of Heat Conduction Equation which Eliminates the Paradox of Instantaneous Propagation, *Comptes Rendus Mathématique*, 247 (1958), pp. 431-433
- [25] Vernotee, P., Les paradoxes de la theorie continue de l equation del la Chaleur, *Comptes Rendus Mathématique*, 246 (1958), pp. 3154-3155
- [26] Christov, C. I., On Frame Indifferent Formulation of the Maxwell-Cattaneo Model of Finite Speed Heat Conduction, *Mechanics Research Communications*, 36 (2009), 4, pp. 481-486
- [27] Straughan, B., Thermal Convection with the Cattaneo-Christov Model, *International Journal of Heat and Mass Transfer*, 53 (2010), 1-3, pp. 95-98
- [28] Tibullo, V., et al., A Uniqueness Result for the Cattaneo-Christov Heat Conduction Model Applied to Incompressible Fluids, *Mechanics Research Communications*, 38 (2011), 1, pp. 77-99
- [29] Han, S., et al., Coupled Flow and Heat Transfer in Viscoelastic Fluid with Cattaneo-Christov Heat Flux Model, *Applied Mathematics Letters*, 38 (2014), Dec., pp. 87-93
- [30] Hayat, T., et al., Impact of Cattaneo-Christov Heat Flux in the Flow over a Stretching Sheet with Variable Thickness, *AIP Advances*, 5 (2015), 8, 087159
- [31] Khan, W. A., et al., Impact of Chemical Processes on 3D Burgers Fluid Utilizing Cattaneo-Christov Double-Diffusion: Applications of Non-Fourier's Heat and Non-Fick's Mass Flux Models, *Journal of Molecular Liquids*, 223 (2016), Nov., pp. 1039-1047
- [32] Hayat, T., et al., Thermally Stratified Stretching Flow with Cattaneo-Christov Heat Flux, *International Journal of Heat and Mass Transfer*, 106 (2017), Mar., pp. 289-294
- [33] Hayat, T., et al., On Doubly Stratified Chemically Reactive Flow of Powell-Eyring Liquid Subject to Non-Fourier Heat Flux Theory, *Results in Physics*, 99 (2017), Dec., pp. 99-106
- [34] Ali, M. E., et al., Cattaneo-Christov Model for Radiative Heat Transfer of Magnetohydrodynamic Casson-Ferrofluid: A Numerical Study, *Results in Physics*, 7 (2016), Nov., pp. 21-30
- [35] Sui, J., et al., Boundary Layer Heat and Mass Transfer with Cattaneo-Christov Double-Diffusion in Upper-Convected Maxwell Nanofluid Past a Stretching Sheet with Slip Velocity, *International Journal of Thermal Science*, 104 (2016), June, pp. 461-468

- [36] Nadeem, S., et al., Impact of Stratification and Cattaneo-Christov Heat Flux in the Flow Saturated with Porous Medium, *Journal of Molecular Liquids*, 224 (2016), Part A, pp. 423-430
- [37] Fairchild, G. W., et al., The Trophic State 'Chain Of Relationships' in Ponds: Does Size Matter?, *Hydrobiologia*, 539 (2005), 1, pp. 35-46
- [38] Mazumder, A., et al., Effects of Fish and Plankton and Lake Temperature and Mixing Depth, *Science*, 247 (1990), 4940, pp. 312-315
- [39] Schindler, D. W., et al., The Effects of Climatic Warming on the Properties of Boreal Lakes and Streams at the Experimental Lakes Area, *Northwestern Ontario, Limnology and Oceanography*, 41 (1996), 5, pp. 1004-1017
- [40] Khan, N. B., et al., Numerical Investigation of the Vortex-Induced Vibration of an Elastically Mounted Circular Cylinder at High Reynolds Number ($Re = 10^4$) and Low Mass Ratio Using the Rans Code, *Plas One*, 12 (2017) 10, e0185832
- [41] Khan, N. B., et al., VIV Study of an Elastically Mounted Cylinder Having Low Mass-Damping Ratio Using Rans Model, *International Journal of Heat and Mass Transfer*, 121 (2018), June, pp. 309-314
- [42] Khan, N. B., et al., Numerical Investigation of Flow Around Cylinder at Reynolds Number = 3900 with Large Eddy Simulation Technique: Effect of Spanwise Length and Mesh Resolution, *Proceedings*, Institution of Mechanical Engineers, Part M: Journal of Engineering for the Maritime Environment, 2018
- [43] Khan, N. B., et al., Numerical Investigation of Vortex-Induced Vibration of an Elastically Mounted Circular Cylinder with One-Degree of Freedom at High Reynolds Number Using Different Turbulent Models, *Proceedings*, Institution of Mechanical Engineers, Part M: Journal of Engineering for the Maritime Environment, 2018
- [44] Gireesha, B. J., et al., Effect of Suspended Nanoparticles on Three-Dimensional MHD Flow, Heat and Mass Transfer of Radiating Eyring-Powell Fluid over a Stretching Sheet, *Journal of Nanofluids*, 4 (2015), 4, pp. 474-484
- [45] Mahanthesh, B., et al., Nonlinear Convective and Radiated Flow of Tangent Hyperbolic Liquid Due to Stretched Surface with Convective Condition, *Results in Physics*, 7 (2017), July, pp. 2404-2410
- [46] Mahanthesh, B., et al., Unsteady Three-Dimensional MHD Flow of a Nano Eyring-Powell Fluid Past a Convectively Heated Stretching Sheet in the Presence of Thermal Radiation, Viscous Dissipation and Joule Heating, *Journal of the Association of Arab Universities for Basic and Applied Sciences*, 23 (2017), June, pp. 75-84
- [47] Gireesha, B. J., et al., Nonlinear 3D Flow of Casson-Carreau Fluids with Homogeneous-Heterogeneous Reactions: A Comparative Study, *Results in Physics*, 7 (2017), Aug., pp. 2762-2770